

# Novel Therapy for Acquired Tracheomalacia with a Tissue-Engineered Extraluminal Tracheal Splint and Autologous Mesenchymal-Derived Chondrocytes

Yaaziel Melgarejo-Ramírez<sup>1\*</sup> Juan C. Ceballos-Cantú<sup>2\*</sup> Eric de J. Montes-Olave<sup>2</sup>   
 Bruno Hernández-Tapia<sup>1</sup> Víctor Rojas-Figueroa<sup>2</sup> Gabriela Ramírez-Arroyo<sup>2</sup>   
 Fabiana Cortés-Acosta<sup>2</sup> Mario Dorantes-Pavón<sup>2</sup> Hugo Lecona-Butrón<sup>3</sup>   
 Olga E. Beltrán-Rodríguez-Cabo<sup>2</sup>

<sup>1</sup>Laboratorio de Biotecnología, Instituto Nacional de Rehabilitación Luis Guillermo Ibarra Ibarra, Ciudad de México, México

<sup>2</sup>Subdirección de Otorrinolaringología, Instituto Nacional de Rehabilitación Luis Guillermo Ibarra Ibarra, Ciudad de México, México

<sup>3</sup>Bioterio y Cirugía Experimental, Instituto Nacional de Rehabilitación Luis Guillermo Ibarra Ibarra, Ciudad de México, México

Address for correspondence Olga E. Beltrán-Rodríguez-Cabo, MD, Subdirección de Otorrinolaringología. Instituto Nacional de Rehabilitación Luis Guillermo Ibarra Ibarra, Calzada México-Xochimilco N° 289. Col. Arenal de Guadalupe. C.P. 14389, México (e-mail: olberoca@hotmail.com; obeltran@inr.gob.mx; ymelgarejo@inr.gob.mx).

Int Arch Otorhinolaryngol 2023;27(2):e342–e350.

## Abstract

**Introduction** Acquired tracheomalacia (ATM) is characterized by a loss of structural strength of the tracheal framework, resulting in airway collapse during breathing. Near half of the patients undergoing prolonged invasive mechanical ventilation will suffer tracheal lesions. Treatment for ATM includes external splinting with rib grafts, prosthetic materials, and tracheal resection. Failure in the use of prosthetic materials has made reconsidering natural origin scaffolds and tissue engineering as a suitable alternative.

**Objective** To restore adequate airway patency in an ovine model with surgically-induced ATM employing a tissue-engineered extraluminal tracheal splint (TE-ETS).

**Methods** In the present prospective pilot study, tracheal rings were partially resected to induce airway collapse in 16 Suffolk sheep (*Ovis aries*). The TE-ETS was developed with autologous mesenchymal-derived chondrocytes and allogenic decellularized tracheal segments and was implanted above debilitated tracheal rings. The animals were followed-up at 8, 12, and 16 weeks and at 1-year postinsertion. Flexible tracheoscopies were performed at each stage. After sacrifice, a histopathological study of the trachea and the splint were performed.

**Results** The TE-ETS prevented airway collapse for 16 weeks and up to 1-year postinsertion. Tracheoscopies revealed a noncollapsing airway during inspiration. Histopathological analyses showed the organization of mesenchymal-derived chondrocytes in lacunae, the proliferation of blood vessels, and recovery of epithelial tissue subjacent to the splint. Splints without autologous cells did not prevent airway collapse.

## Keywords

- ▶ airway splint
- ▶ tracheomalacia
- ▶ tissue engineering
- ▶ respiratory disorder
- ▶ extraluminal splint
- ▶ prostheses and implants

\* Both authors contributed equally for the present work.

received  
November 11, 2021  
accepted after revision  
March 1, 2022

DOI <https://doi.org/10.1055/s-0042-1746194>.  
ISSN 1809-9777.

© 2022. Fundação Otorrinolaringologia. All rights reserved.  
This is an open access article published by Thieme under the terms of the Creative Commons Attribution-NonDerivative-NonCommercial-License, permitting copying and reproduction so long as the original work is given appropriate credit. Contents may not be used for commercial purposes, or adapted, remixed, transformed or built upon. (<https://creativecommons.org/licenses/by-nc-nd/4.0/>)  
Thieme Revinter Publicações Ltda., Rua do Matoso 170, Rio de Janeiro, RJ, CEP 20270-135, Brazil

**Conclusion** It is possible to treat acquired tracheomalacia with TE-ETS without further surgical removal since it undergoes physiological degradation. The present study supports the development of tissue-engineered tracheal substitutes for airway disease.

## Introduction

Acquired tracheomalacia (ATM) is characterized by a loss of structural strength of the anterolateral tracheal framework. It produces a dynamic obstruction due to airway collapse during breathing, causing inefficient secretion clearance, stridor, respiratory distress, and even death. Intubation, trauma, neoplasms, and autoimmune diseases are frequent causes. The true prevalence of the disease is unknown, but in patients undergoing tracheoscopy, the incidence ranges from 1 to 23%.<sup>1</sup> In cases of severe tracheomalacia, mortality is as high as 80%.<sup>2</sup> Current treatment options include management with continuous positive airway pressure (CPAP),<sup>3</sup> extraluminal splinting with rib grafts or prosthetic materials,<sup>4</sup> intraluminal silicone, metal stents,<sup>5</sup> and tracheal resection with end-to-end anastomosis.<sup>6</sup> These are either partial solutions or are highly morbid and are not always suitable for critically ill patients. In the field of tissue engineering, scaffolds should be biocompatible, biodegradable, nonimmunogenic, and possess biomechanical strength.<sup>7</sup> So, current trends focus on tracheal substitution,<sup>8</sup> which might be accomplished through allotransplantation,<sup>9</sup> autologous tissue reconstruction,<sup>10</sup> aortic homograft reconstruction,<sup>11</sup> and tissue engineering.<sup>12,13</sup> High hopes were placed on the latter, but premature clinical translation and failure were a setback. Further preclinical studies are needed to ensure safety and efficacy before clinical translation. Natural-origin scaffolds have been reconsidered as an alternative able to fulfill the characteristic of an ideal splint. In the present work, a tissue-engineered extraluminal tracheal splint (TE-ETS) was created using a decellularized cadaveric trachea, seeded with mesenchymal stromal cell-derived chondrocytes (oMS-DC). The main objective was to restore adequate airway patency in an ovine model with surgically induced ATM employing a TE-ETS. The degree of integration of the splint into the surrounding tissues and the role of the cells seeded to the splint scaffold in the reconstitution of reparative tissue was also investigated.

## Methods

### Ethics

The Institutional Animal Care and Use Committee (RLFSA: AUT-B-A-0315-20) approved all procedures under protocol number INRLGII-50/14. Institutional collaboration included the Otolaryngology Department, the Biotechnology Laboratory, and the animal surgery unit for animal care.

### Chondrogenic Differentiation and Generation of a Novel TE-ETS

Ovine mesenchymal cells (oMSCs) were obtained from epiploic adipose tissue. The cells were isolated by digestion with type II collagenase (3 mg/mL). Stromal-vascular fraction

(SVF) cells were cultured in supplemented medium (DMEM-F12; 10% FBS; 1% penicillin-streptomycin) and non-adherent cells were removed. Cell viability was determined using a Live/Dead kit (Invitrogen, Waltham, MA, USA), proliferation was analyzed via immunolabeled monoclonal antibody against Ki67 (1:50; Santa Cruz, Dallas, Texas, United States), and clonogenic capacity was evaluated using a low-density culture and crystal violet staining. Chondrogenic differentiation was induced in high-density cultures using conditioned media enriched with growth factors (Dulbecco Modified Eagle Medium/Nutrient Mixture F-12 [DMEM-F12,] 10 ng/mL transforming growth factor  $\beta$ 1 [TGF- $\beta$ 1], 1.0 mg/mL insulin, 10 mM dexamethasone, 20 mg/mL ascorbic acid, 1% FBS and 1% penicillin-streptomycin) for 21 days. Differentiation was evaluated in vitro and performed at large-scale culture for splint implantation following the same protocol.<sup>14</sup> Cadaveric heterologous tracheal segments (5–8 cm) were treated with 2 to 6 decellularization cycles (1% trypsin-EDTA for 5 hours at 37°C, 10% guanidine-Tris overnight, sonication in 4% sodium deoxycholate for 3 hours, 1% sodium dodecyl sulfate overnight, and 10 mg/mL DNase type I for 2 hours at 37°C). The DNA content was evaluated in histological sections by nucleus staining with DAPI. The mechanical properties of heterologous tracheal segments were continuously evaluated by participant surgeons. For novel TE-ETS generation, decellularized segments were ensheathed with oMS-DC embedded at  $4 \times 10^7$  cells/mL in medical-grade fibrin hydrogels as the cell carrier biomaterial. Differentiated cells were applied onto the surface of the splint and allowed to polymerize during implantation surgery.

### Animal Care and Perioperative Technique

Sixteen 12-month-old female Suffolk sheep (*Ovis aries*) with an average weight between 25 and 60 kg were used. In all procedures, acepromazine maleate (0.05 mg/kg IV) and propofol (5 mg/kg, IV, PLOFED-20) were administered for sedation before endotracheal intubation. General anesthesia was maintained with isoflurane 3.0% and 3 l/min oxygen. Perioperative care consisted of an intramuscular (IM) antibiotic, either enrofloxacin (5.0 mg/kg for 5 days) or clindamycin-gentamycin (2.5 mg/kg for 5 days), the IM analgesic dipyrone (50 mg/kg for 5 days), and the IM antihistamine diphenhydramine (1.0 mg/kg single dose). The animals were extubated and moved to individual pens for close surveillance and antibiotic therapy until the 4<sup>th</sup> day, when they rejoined the herd.

### Ovine Model for Induced Tracheomalacia and Airway Collapse

Under general anesthesia, the trachea was exposed and 70% of the cartilage circumference from the 3<sup>rd</sup> to the 6<sup>th</sup> tracheal

rings was resected until airway collapse was visible. The mucosa was not injured. To avoid fibrosis, the resected area was covered with a 2.0 mm-thick medical-grade silicone sheet. Tracheoscopies were performed to confirm airway collapse.<sup>15</sup>

### Surgical Insertion of TE-ETS, Postoperative Evaluation, and Sacrifice

Four weeks after ATM induction, the TE-ETS was surgically implanted into each subject through a standardized procedure. The trachea was exposed via a midline cervical incision, the silicone sheet was removed, and the area was debrided and covered with a layer of fibrin hydrogel-embedded differentiated cells. The splint was fitted and sutured to the ATM area and covered with the second layer of cells. The experimental models ( $n = 16$ ) were divided into 3 groups according to the follow-up time: Group I (8 weeks postinsertion [WPIs]), Group II (12 WPIs), and Group III (16 WPIs). One specimen was kept in observation for 1 year after insertion. To analyze the role differentiated chondrogenic cells play in tissue regeneration, scaffolds without cells were implanted in three subjects, which were distributed evenly in Groups I, II, and III. During follow-up, the animals were monitored for clinical signs of inflammation or rejection and serial tracheoscopies were performed. After completing the pre-established follow-up period, the models were sacrificed by IV pentobarbital overdose (70 mg/kg), and the TE-ETS were removed. Tissues were fixed in 4% paraformaldehyde and embedded in paraffin, and histological slices were stained with safranin O for analysis of the cartilage and proteoglycans.

### Statistical and Cellular Analysis

Group comparisons were made by *t*-tests (2 groups) or by one-way analysis of variance (ANOVA) with posthoc test ( $> 2$  groups). *P*-values  $< 0.05$  were considered significant. All quantitative data are expressed as means and standard deviations (SDs). Cell percentages were calculated by counting individual cells in at least five fields per experiment. GraphPad Prism (GraphPad Software, San Diego, CA, USA) was used for statistical analysis.

## Results

### Extraluminal Tracheal Splint in Biocompatible with Autologous Mesenchymal Cell-Derived Chondrocytes

Ovine adipose tissue allowed isolation of adherent cells from stromal-vascular fraction (SVF) 24 hours after cell seeding. Primary adipose-derived oMSCs exhibited fibroblast morphology (**Fig. 1a**) and colony-forming capacity after 2 days in monolayer culture. By day 5, the colonies had between 50 and 250 cells/colony (**Fig. 1b**). Cell viability was  $95.7 \pm 1.1\%$  after 7 days in culture (**Figs. 1c** and **g**). Cell proliferation, measured by the expression of Ki67, was detected in 7.5% of the cells in the early phase of primary culture (**Figs. 1d** and **h**). Ovine mesenchymal cells-derived chondrocytes changed from spindle to polygonal shape and displayed aggregate formation nodules that increased in size over the differentiation period. Glycosaminoglycans (GAGs) in the cell cytoplasm and matrix stained positively by Alcian blue (**Fig.**

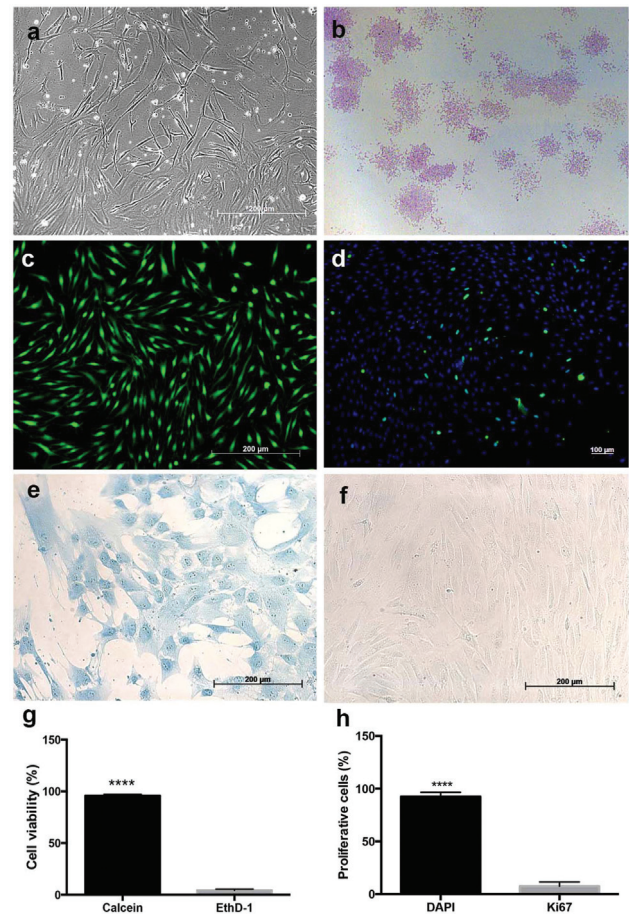


**Fig. 1** Isolation and differentiation of ovine mesenchymal-derived chondrocytes. Ovine mesenchymal stromal cells (oMSC) exhibited fibroblast morphology (a). Colonies of oMSC increased in number by day 5 (b). Cell viability was  $95.7\% \pm 1.1$  after 7 days culture (c and g). Cell proliferation was detected in 7.5% of cells in the early phase of primary culture (d and h). Glycosaminoglycans positively stained in cell cytoplasm and matrix by alcian blue during chondrogenic induction after 21 days (e). Nonstimulated cells did not display significant changes. Scale bars equivalent to 200  $\mu$ m (a, c, e, and f) and 100  $\mu$ m (d).

**1e**). Nonstimulated cells did not display significant changes, aggregation, or positive staining, but cell growth was similar to that of oMSCs (**Fig. 1f**).

DAPI staining was performed to verify the absence of DNA content in cadaveric heterologous tracheal segments. Staining the nontreated tracheal cartilage detected DNA in the chondrocyte nuclei and in the connective tissue that ensheathes the cartilage (**Fig. 2a**). After two cycles of decellularization, the DNA content gradually reduced (**Figs. 2b** and **c**). After three cycles, the DNA content was degraded, leaving residue on the inner parts of the tissue that was positive to DAPI staining (**Fig. 2d**). Chondral lacunae were visibly absent of chondrocytes or nuclei compared with the untreated trachea (**Fig. 2e**). The tracheal segments underwent a considerable reduction of proteoglycans, but the extracellular matrix (ECM) structure of cartilage was maintained except for the connective tissue and soft muscle that joins the cartilaginous rings (**Fig. 2f**). In general, three decellularization cycles resulted in the elimination of



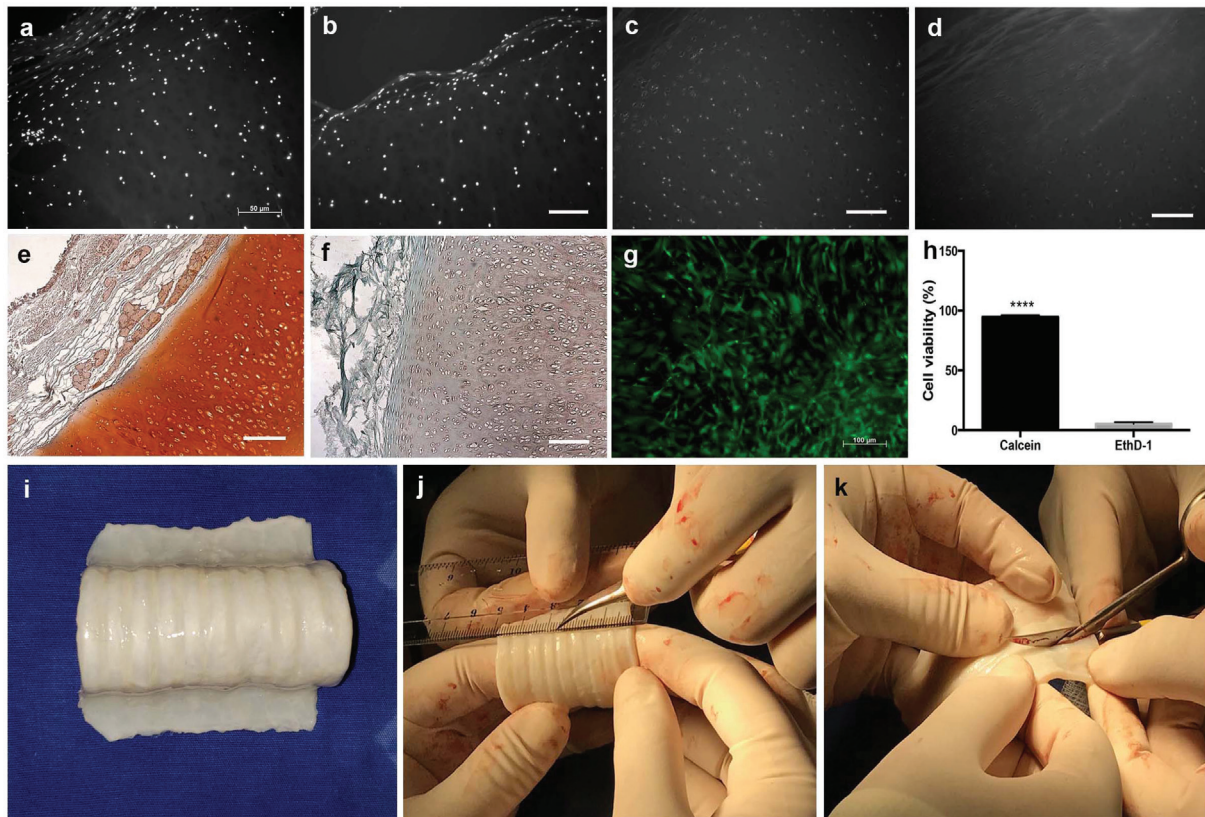


**Fig. 2** Decellularization of extraluminal tracheal splints and hydrogel culture of oMSC-derived chondrocytes. DNA content in histological slices of untreated heterologous tracheal segments (a). After decellularization, the DNA content gradually reduced (b-c-d). Safranin O staining revealed proteoglycans found in ECM in native tracheal cartilage (e) and their reduction after three decellularization cycles (f). Ovine MSC-derived chondrocytes embedded in fibrin hydrogels showed 94.7% cell viability after 7 days culture (h). Decellularization resulted in the elimination of undesired connective tissue layers while maintaining rigidity and flexibility of the tracheal segment allowing manipulation and size adjustment (i-k). Scale bars 50  $\mu$ m (a-f) and 100  $\mu$ m (g).

undesired connective tissue layers while maintaining the rigidity and flexibility of the tracheal segment, allowing manipulation and size adjustment. Further cycles led to a loss of ECM integrity, and even separation of cartilaginous rings, compromising the functionality of the extraluminal splint (**Fig. 2i-k**). Ovine mesenchymal cells-derived chondrocytes were embedded in fibrin hydrogels to allow cell growth and cellular adhesion to the splint scaffold. It was possible to observe viable chondrocytes developing a polygonal shape similar to that displayed in the high-density cultures. The viability of the cells in the hydrogel-embedded chondrocytes was 94.7% after 7 days of culture (**Fig. 2h and g**).

### Partial Cartilage Resection Causes Airway Collapse in an Ovine Model

A standardized animal model of induced tracheomalacia was obtained via full-thickness removal of 70% of the circumference of 5 tracheal rings, avoiding mucosal injury (**Fig. 3a, 3b**). Removal of five rings caused dyspnea at rest and audible stridor, hence the number of tracheal rings resected was reduced to four, which was still sufficient to produce airway collapse (**Fig. 3c, 3d**). Dyspnea with exertion was evident in all subjects (**Fig. 3d and e**), so it was considered an appropriate tracheomalacia model. Before the TE-ETS was

surgically implanted, the persistence of airway collapse in each tracheomalacia model was verified with a tracheoscopy.

### Engineered Extraluminal Splint Restores Airway Patency and Promotes Tissue Regeneration

When the TE-ETS was implanted above the malacic area, it adopted the tubular shape of the trachea and was easy to handle (**Fig. 4a**). Fibrin-embedded oMS-DC favored fixation of the TE-ETS to the malacic site (**Fig. 4b**). None of the animals had clinical signs of inflammation or rejection, including fever, anorexia, or abnormal behavior after surgery. All treated animals ( $n = 16$ ) survived after insertion of the TE-ETS. A final tracheoscopy performed before sacrifice showed no airway collapse during inspiration, and lumen constriction due to fibrosis was  $< 10\%$ . In-vivo airway collapse was not evident even after applying mild manual pressure over the treated area. In some animals, fibrotic rings formed around the splint, but the airway was not compromised (**Fig. 4c**). The TE-ETS showed vascular organization, allowing the airway to recover function. All splints were found in place, surrounded by fibrous tissue; this made the splint harder than when implanted, but it was still elastic (**Fig. 4d and e**). No major macroscopic differences were seen between the splints amongst the different groups (**Fig. 4f**).

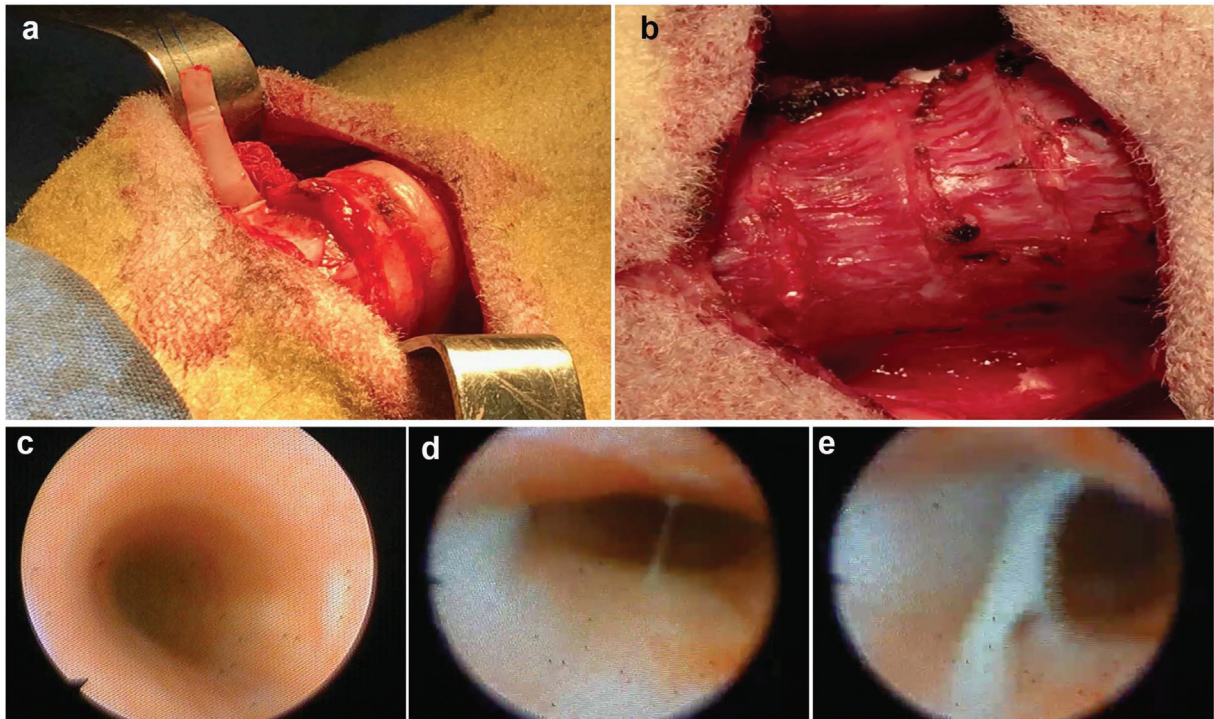


**Fig. 3** Ovine model for acquired tracheomalacia (ATM). Full-thickness removal of 70% of the circumference of the 3<sup>rd</sup> to the 6<sup>th</sup> tracheal rings, respecting the mucosa (a-b). Tracheoscopy showed absence of airway collapse in healthy animals (c). In contrast, airway collapse was shown in ovine models with ATM; formation of mucus was evident (d-e).

Animals implanted with a decellularized scaffold without oMS-DC showed persistence of tracheal collapse during inspiration. After sacrifice, the splints induced a low inflammatory infiltrate, displayed a breach from the contiguous connective tissue without edema, and had unstable tissue constitution adjacent to the lesion (►Fig. 5 panel a). After 8 WPIs, TE-ETSs were properly positioned above the ATM area and subjacent tissue showed areas of mineralization accompanied by an inflammatory infiltrate with predominance of lymphocytes and histiocytes. Fibrosis zones contained abundant deposits of collagen mainly constituted by fibroblasts with barely perceptible nuclei. Safranin O staining revealed adequate decellularization of the external splint compared with tracheal cartilage (►Fig. 5 panel b). After 12 WPIs, airway collapse decreased but was still detectable. Staining revealed that the inflammatory infiltrate resolved and there were no areas of osseous metaplasia or granulomas. Areas with steatonecrosis and ossification were not considerable, and tissue subjacent to the extraluminal tracheal splints showed a dense constitution. The TE-ETS had no proteoglycans, following previous decellularization findings. It is also noteworthy that we detected organization of oMS-DC in lacunae and proliferation of blood vessels in tissue subjacent to the TE-ETS (►Fig. 5 panel c). For models sacrificed at 16 WPI, tracheal collapse significantly decreased. Granulomas and considerable inflammatory infiltrate were absent, while mineralization, cytonecrosis, osteonecrosis, ossification, or metaplastic changes also resolved. Tissue underlying implanted areas presented neof ormation of ECM, containing oMS-chondrocyte aggregates (►Fig. 5 panel d). Remarkably, in the animal

that was kept under observation for 1 year after splint insertion, tracheal collapse was not detected, and the tracheal diameter resembled that of uninjured animals. Slow degradation of the splint scaffold was noticeable; nevertheless, a remarkable regeneration of ECM in ATM areas was observed, which restored the mechanical strength of the trachea. The respiratory epithelium suffered changes after ATM induction, but it recovered in both models implanted with the acellularized splints and those that received the TE-ETSs. The vascularization, reconstitution, and inner layer of the tracheal mucosa were most evident 1 year postinsertion (►Fig. 5 panel e). In all cases, autologous cells promoted adherence and tissue regeneration between the TE-ETS and ATM zones.

## Discussion

More traditional treatments for ATM, such as intraluminal splints, have had discouraging results. Complex surgical procedures are associated with a high risk of complications, such as anastomosis, dehiscence, and wound infection. Tracheal replacement methods that do not involve tissue engineering include allogeneic transplantation, autologous tissue reconstruction, and aortic homograft reconstruction; however, currently, there is still no ideal tracheal substitute.<sup>8</sup> Unresolved problems include mucociliary clearance, poor vascular nutrition to the neotrachea, and the need for immunosuppression. In the present study, we were able to overcome these issues by developing a TE-ETS that has the ideal splint properties of being malleable, nonimmunogenic, and absorbable, as well as promoting neotissue formation.<sup>16</sup>



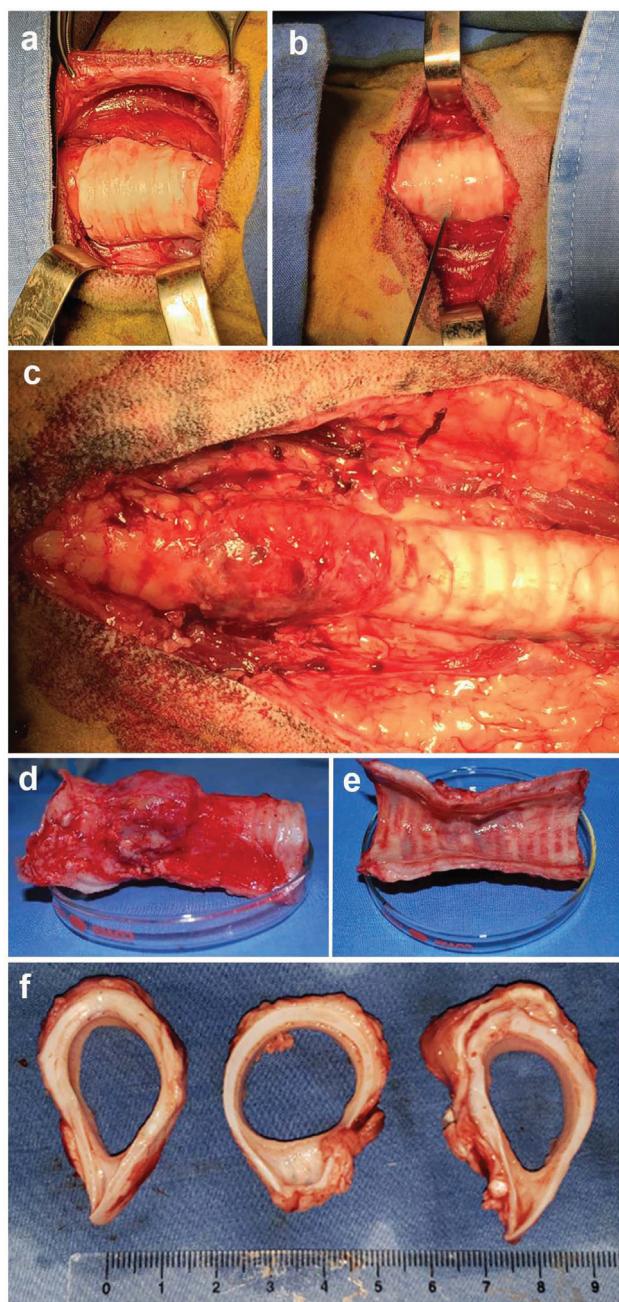


**Fig. 4** Surgical implantation of the tissue engineered extraluminal tracheal splint (TE-ETS). The malacic area was exposed and the TE-ETS was implanted (a). Ovine mesenchymal cells-derived chondrocytes embedded in medical grade fibrin hydrogels at a cell density of  $4 \times 10^7$  cells/mL were applied onto the TE-ETS (b). After the follow-up was completed, the animals were sacrificed, and the implanted splints were extracted and fixed for histological analysis (c-f).

The two main components are the splint and the oMS-derived chondrocytes seeded to the splint. The former provides support, avoids mechanical stress, and reduces airway collapse, while the latter promotes the formation of connective tissue and cartilage islets that improve mechanical support in the ATM area. Once the splint is absorbed, the newly developed cartilage remains and prevents airway collapse. Ovine mesenchymal cells that met the criteria described for mesenchymal stromal cells (MSC) by the

International Society for Cellular Therapy<sup>17</sup> were obtained. These cells achieved the multipotency potential reported for oMSC from peripheral blood,<sup>18</sup> human adipose-derived MSCs, and endometrium.<sup>19</sup> Chondrogenic differentiation potential based on GAGs production and cell proliferation rate were also comparable to human MSC.<sup>20</sup> Hence, ovine adipose-derived MSCs retain the ability to differentiate and fulfill requirements for tissue engineering models. The mechanical properties of the decellularized trachea have been demonstrated to have similar biomechanical profiles to the native trachea.<sup>21</sup> Another advantage of decellularized trachea is that their microstructure plays an important role in neotissue formation through chemoattraction, cell support, and signaling.<sup>22</sup> Most studies have their endpoints established in < 90 days, including poly-ε-caprolactone (PCL) 3D-printed materials, whereas our sheep were kept alive up to 1 year after implantation. This longer period of observation allowed us to explore how the TE-ETS integrated into the tissue and the risk of producing stenosis on a long-term basis. Additionally, most of the trials using PCL 3D-printed materials were completed before absorption, a process that takes between 2 and 3 years. Therefore, it is not possible to analyze if airway collapse could be prevented solely by neotissue formation after the splint was absorbed.<sup>23</sup> It will be interesting to compare the outcomes of PCL versus decellularized splints, with and without cellular components, especially on a long-term basis. An alternative to produce the splint was 3D printing; however, despite progress made with 3D printing technology, it is recognized that the development of improved biomaterials and imaging techniques is still required to increase the applicability of 3D printed devices.<sup>24</sup>

The combination of biological, chemical, and physical agents for the disruption of cell membranes improved the dynamic decellularization of allogenic tracheal segments after three cycles while preserving the main constituents of ECM. This process removes adventitia, blood vessels, and internal mucosal folds. This is relevant because the MHC molecules that are responsible for immunogenicity reside in noncartilaginous tissue.<sup>25</sup> Based on the fact that elimination of heterologous DNA reduces the immunological response of the host,<sup>26</sup> our strategy included the addition of autologous oMS-chondrocytes to minimize immune response. As proof, the animals showed no signs of rejection after implanting the splints, despite receiving no immunosuppression.

The scaffold can be adapted to lesion requirements at the moment of surgical implantation. In our model, hydrogel-embedded oMS-chondrocytes formed a cellular layer onto the malacic site, facilitating fixation and immobilization of the splint to the debilitated area. A logistical advantage of this model is that cells can be taken directly from the cell culture facility to the operating room, where they are seeded. Another advantage is that production times are optimized; for example, a TE-ETS is fully developed for implantation in < 8 weeks, but when previously differentiated autologous cells are used, the estimated development time is 2 weeks.

Traditionally, rabbits have been used as models of tracheal airway collapse because the diameter and elasticity<sup>27</sup> of their trachea are similar to that of the human pediatric trachea.



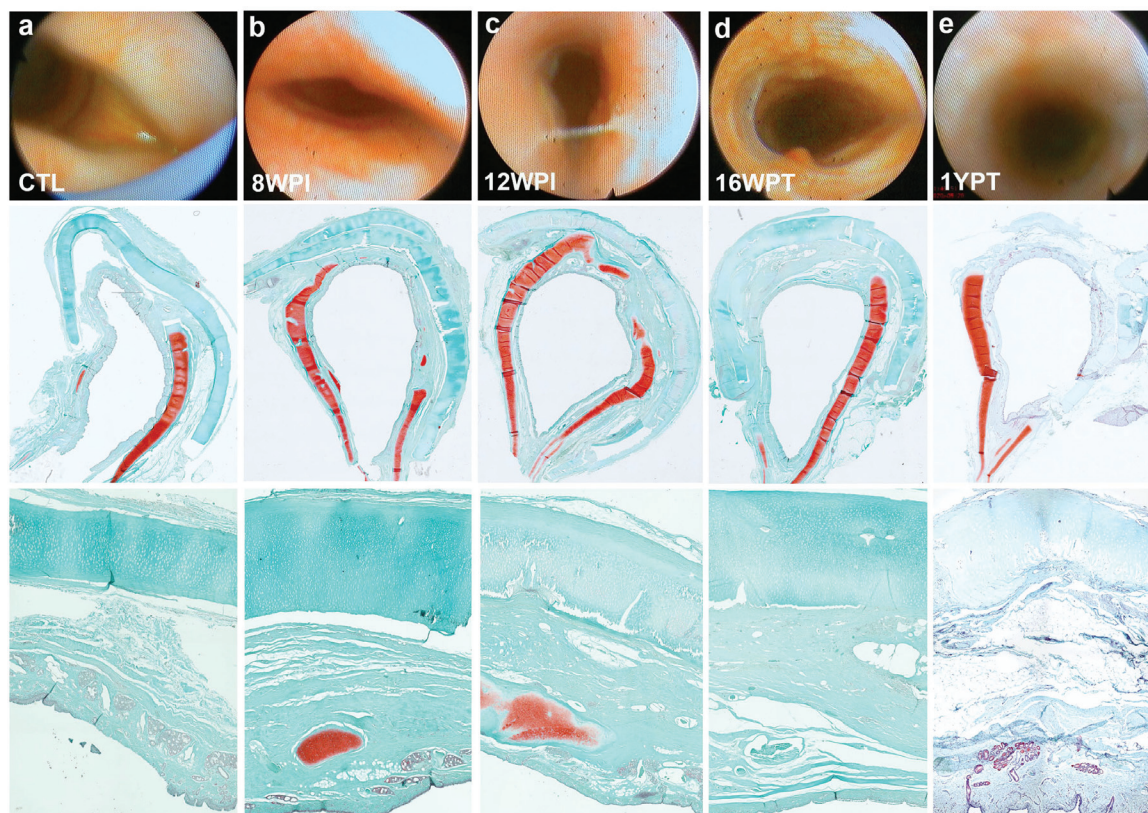


**Fig. 5** Engineered extraluminal splint restores airway patency. Animals implanted with a decellularized scaffold without oMSC-chondrocytes showed persistence of tracheal collapse during inspiration. The decellularized splint showed evident separation from the contiguous connective tissue without formation of edema, according to safranin O staining (a). For the TE-ETS, airway collapse persisted 8 weeks postimplant (8WPIs). Fibrosis zones with abundant deposits of collagen constituted by fibroblasts were evident (b). After 12 WPIs, airway collapse decreased but was still detectable. Absence of chronic inflammatory infiltrate, organization of oMSC-derived chondrocytes in lacunae and proliferation of blood vessels in tissue subjacent to the TE-ETS were evident changes (c). For models sacrificed at 16 WPIs, collapse significantly decreased. Tissue underlying implanted areas presented neof ormation of ECM containing oMSC-derived chondrocytes (d). In the animal kept alive 1 year postimplant, tracheal collapse was not detected and tracheal diameter resembled that of uninjured animals. Regeneration of ECM in ATM areas that were beneath the TE-ETS (e).

However, in adulthood, rabbits have almost complete tracheal rings, making this model unsuitable for our study.<sup>28,29</sup> Ovine, canine, and porcine models are more accurate models of the human adult trachea. The treatment of ATM with the TE-ETS developed in the present study does not require immunosuppression, can create an appropriate vascular network, preserves mucociliary clearance, and its implantation in the patient is technically simple.

The postoperative follow-up revealed fibrosis from 8 WPIs that increased by 12 WPIs and finally decreased by 16 WPIs. This fibrosis is considered the initial phase for regeneration of an ECM rich in collagen type I and type II and does not seem to produce tracheal stenosis; however, further studies have to be performed to better understand its significance. It was possible to determine early signs of tissue vascularization in the TE-ETS starting from 8 WPIs and until 16 WPIs.

Although we previously performed *in vitro* differentiation, it was uncertain if the microenvironment influenced cell phenotype. The histological analysis revealed the formation of chondrogenic nodules that showed cell organization and proteoglycan synthesis attributable to autologous oMSC-

chondrocytes that were seeded during the implantation. This effect confirms that, in our model, the chondrogenic pre-differentiation of oMSC using TGF- $\beta$ 1 can be chondrogenically-primed oMSC and promote *in vivo* chondrogenesis.<sup>19</sup>

Other research groups using animal models have resected between 8 and 10 tracheal rings, producing cyanosis and stridor in the postoperative period.<sup>30,31</sup> We decided to remove four rings to cause the airway collapse that defines tracheomalacia at the same time as ensuring that the animals presented with dyspnea and stridor only during exertion. This measure was considered humane, but it also represents a limitation of our study, since the sheep in our model had no severe clinical manifestations, as has been shown in other studies.<sup>32</sup> It is important to recognize that this splint was designed for the management of tracheomalacia and not as a universal tracheal substitute. In tracheomalacia, the mucosal epithelial lining is healthy, and only the structural rigidity of the external framework is affected.<sup>33</sup> The splint restores the lost structural rigidity of the airway, but it does not produce major luminal changes. Therefore, it is not indicated for clinical situations that require tracheal substitution, such as severe tracheal stenosis or extensive malignant neoplasms.

## Conclusion

The TE-ETS developed prevents airway collapse and promotes chondrogenesis. Furthermore, it does not require exposure of the internal airway to the external environment, preserving mucociliary clearance. The TE-ETS fulfills several characteristics of the ideal stent: it is biocompatible, non-immunogenic, has an appropriate degradation rate, is easily available at a low cost, is easy to implant, and does not obstruct the airway in our ATM animal model.

### Funding

This project was supported by Consejo Nacional de Ciencia y Tecnología (CONACYT) in Mexico. Grants Conacyt FOSISS SALUD-2014-01-234406, SALUD-2015-01-262404. The project was also supported by Instituto Nacional de Rehabilitación Luis Guillermo Ibarra Ibarra.

### Conflict of Interests

The authors have no conflict of interests to declare.

### Acknowledgments

We would like to acknowledge Dra. Cristina Velasquillo and Dra. Bárbara Luján for administrative support. Hiram García Campillo Zootechnical veterinary doctor (ZVD), Ricardo Mejenez López ZVD, Javier Pérez Gallaga ZVD, from Bioterio y Cirugía Experimental. Also Biol. Exp. Ana Karen Olmos, M. en C. Noé Zacauala from Laboratorio de Biotecnología for the imaging acquisition and technical support. Biol. Julieta García for histological techniques; IQ. Karina Martínez and Tec. Lab. Xóchitl Guerrero for technical support.

## References

- Aquino SL, Shepard JA, Ginns LC, et al. Acquired tracheomalacia: detection by expiratory CT scan. *J Comput Assist Tomogr* 2001;25(03):394–399. Doi: 10.1097/00004728-200105000-00011
- Mitchell ME, Rumman N, Chun RH, et al. Anterior tracheal suspension for tracheobronchomalacia in infants and children. *Ann Thorac Surg* 2014;98(04):1246–1253. Doi: 10.1016/j.athoracsur.2014.05.027
- Carden KA, Boiselle PM, Waltz DA, Ernst A. Tracheomalacia and tracheobronchomalacia in children and adults: an in-depth review. *Chest* 2005;127(03):984–1005. Doi: 10.1378/chest.127.3.984
- Cho JH, Kim H, Kim J. External tracheal stabilization technique for acquired tracheomalacia using a tailored silicone tube. *Ann Thorac Surg* 2012;94(04):1356–1358. Doi: 10.1016/j.athoracsur.2012.04.133
- Chen G, Wang Z, Liang X, et al. Treatment of cuff-related tracheal stenosis with a fully covered retrievable expandable metallic stent. *Clin Radiol* 2013;68(04):358–364. Doi: 10.1016/j.crad.2012.08.022
- Kirschbaum A, Teymoortash A, Suárez C, et al. Treatment of large tracheal defects after resection: Laryngotracheal release and tracheal replacement. *Auris Nasus Larynx* 2016;43(06):602–608. Doi: 10.1016/j.anl.2016.03.009
- Fishman JM, Lowdell M, Birchall MA. Stem cell-based organ replacements-airway and lung tissue engineering. *Semin Pediatr Surg* 2014;23(03):119–126. Doi: 10.1053/j.sempedsurg.2014.04.002
- Udelsman B, Mathisen DJ, Ott HC. A reassessment of tracheal substitutes—a systematic review. *Ann Cardiothorac Surg* 2018;7(02):175–182. Doi: 10.21037/acs.2018.01.17
- Delaere PR, Vranckx JJ, Meulemans J, et al. Learning curve in tracheal allotransplantation. *Am J Transplant* 2012;12(09):2538–2545. Doi: 10.1111/j.1600-6143.2012.04125.x
- Fabre D, Kolb F, Fadel E, et al. Successful tracheal replacement in humans using autologous tissues: an 8-year experience. *Ann Thorac Surg* 2013;96(04):1146–1155. Doi: 10.1016/j.athoracsur.2013.05.073
- Davidson MB, Mustafa K, Girdwood RW. Tracheal replacement with an aortic homograft. *Ann Thorac Surg* 2009;88(03):1006–1008. Doi: 10.1016/j.athoracsur.2009.01.044
- Elliott MJ, Butler CR, Varanou-Jenkins A, et al. Tracheal Replacement Therapy with a Stem Cell-Seeded Graft: Lessons from Compassionate Use Application of a GMP-Compliant Tissue-Engineered Medicine. *Stem Cells Transl Med* 2017;6(06):1458–1464. Doi: 10.1002/sctm.16-0443
- Macchiarini P, Jungebluth P, GoT, et al. Clinical transplantation of a tissue-engineered airway. *Lancet* 2008;372(9655):2023–2030. Doi: 10.1016/S0140-6736(08)61598-6
- Rentsch C, Hess R, Rentsch B, et al. Ovine bone marrow mesenchymal stem cells: isolation and characterization of the cells and their osteogenic differentiation potential on embroidered and surface-modified polycaprolactone-co-lactide scaffolds. *In Vitro Cell Dev Biol Anim* 2010;46(07):624–634
- Tsukada H, O'Donnell CR, Garland R, Herth F, Decamp M, Ernst A. A novel animal model for hyperdynamic airway collapse. *Chest* 2010;138(06):1322–1326. Doi: 10.1378/chest.10-0165
- Kojima K, Vacanti CA. Tissue engineering in the trachea. *Anat Rec (Hoboken)* 2014;297(01):44–50. Doi: 10.1002/ar.22799
- Dominici M, Le Blanc K, Mueller I, et al. Minimal criteria for defining multipotent mesenchymal stromal cells. The International Society for Cellular Therapy position statement. *Cytherapy* 2006;8(04):315–317. Doi: 10.1080/14653240600855905
- Lyahyai J, Mediano DR, Ranera B, et al. Isolation and characterization of ovine mesenchymal stem cells derived from peripheral blood. *BMC Vet Res* 2012;8(01):169. Doi: 10.1186/1746-6148-8-169
- Hwang NS, Im SG, Wu PB, et al. Chondrogenic priming adipose-mesenchymal stem cells for cartilage tissue regeneration. *Pharm Res* 2011;28(06):1395–1405. Doi: 10.1007/s11095-011-0445-2
- Haddouti E-M, Randau TM, Hilgers C, et al. Characterization and Comparison of Human and Ovine Mesenchymal Stromal Cells from Three Corresponding Sources. *Int J Mol Sci* 2020;21(07):E2310. Doi: 10.3390/ijms21072310
- Chiang T, Pepper V, Best C, Onwuka E, Breuer CK. Clinical Translation of Tissue Engineered Trachea Grafts. *Ann Otol Rhinol Laryngol* 2016;125(11):873–885. Doi: 10.1177/0003489416656646
- Badylak SF. The extracellular matrix as a biologic scaffold material. *Biomaterials* 2007;28(25):3587–3593. Doi: 10.1016/j.biomaterials.2007.04.043
- Chan DS, Fnaiss N, Ibrahim I, Daniel SJ, Manoukian J. Exploring polycaprolactone in tracheal surgery: A scoping review of in-vivo studies. *Int J Pediatr Otorhinolaryngol* 2019;123:38–42. Doi: 10.1016/j.ijporl.2019.04.039
- Morrison RJ, Hollister SJ, Niedner MF, et al. Mitigation of tracheobronchomalacia with 3D-printed personalized medical devices in pediatric patients. *Sci Transl Med* 2015;7(285):285ra64. Doi: 10.1126/scitranslmed.3010825
- Zang M, Zhang Q, Chang EI, Mathur AB, Yu P. Decellularized tracheal matrix scaffold for tissue engineering. *Plast Reconstr Surg* 2012;130(03):532–540. Doi: 10.1097/PRS.0b013e31825dc084
- Zang M, Zhang Q, Chang EI, Mathur AB, Yu P. Decellularized tracheal matrix scaffold for tracheal tissue engineering: in vivo host response. *Plast Reconstr Surg* 2013;132(04):549e–559e. Doi: 10.1097/PRS.0b013e3182a013fc
- McGill M, Raol N, Gipson KS, et al. Preclinical assessment of resorbable silk splints for the treatment of pediatric tracheomalacia. *Laryngoscope* 2019;129(09):2189–2194. Doi: 10.1002/lary.27540



- 28 ten Hallers EJO, Rakhorst G, Marres HAM, et al. Animal models for tracheal research. *Biomaterials* 2004;25(09):1533–1543. Doi: 10.1016/s0142-9612(03)00500-3
- 29 Gorostidi F, Courbon C, Burki M, Reinhard A, Sandu K. Extraluminal biodegradable splint to treat upper airway anterior malacia: A preclinical proof of principle. *Laryngoscope* 2018;128(02):E53–E58. Doi: 10.1002/lary.26857
- 30 Okamoto T, Yamamoto Y, Gotoh M, et al. Slow release of bone morphogenetic protein 2 from a gelatin sponge to promote regeneration of tracheal cartilage in a canine model. *J Thorac Cardiovasc Surg* 2004;127(02):329–334. Doi: 10.1016/j.jtcvs.2003.08.017
- 31 Zopf DA, Flanagan CL, Wheeler M, Hollister SJ, Green GE. Treatment of severe porcine tracheomalacia with a 3-dimensionally printed, bioresorbable, external airway splint. *JAMA Otolaryngol Head Neck Surg* 2014;140(01):66–71. Doi: 10.1001/jamaoto.2013.5644
- 32 Les AS, Ohye RG, Filbrun AG, et al. 3D-printed, externally-implanted, bioresorbable airway splints for severe tracheobronchomalacia. *Laryngoscope* 2019;129(08):1763–1771. Doi: 10.1002/lary.27863
- 33 Law JX, Liao LL, Aminuddin BS, Ruzzymah BHI. Tissue-engineered trachea: A review. *Int J Pediatr Otorhinolaryngol* 2016;91:55–63. Doi: 10.1016/j.ijporl.2016.10.012